

## An electrical extension of automata-based heart models for closed-loop validation of pacemakers

Gabriel V.N. Magalhães\* Gutemberg G. Santos Jr.\*\*  
Antonio M.N. Lima\*\*\*

\* Programa de Pós-Graduação em Engenharia Elétrica - PPgEE  
Centro de Engenharia Elétrica e Informática - CEEI  
Universidade Federal de Campina Grande - UFCG  
(e-mail: gabriel.magalhaes@ee.ufcg.edu.br).

\*\* Departamento de Engenharia Elétrica - DEE, CEEI, UFCG  
(e-mail: gutemberg@dee.ufcg.edu.br)

\*\*\* DEE, PPgEE, CEEI, UFCG  
(e-mail: amnlima@dee.ufcg.edu.br)

---

**Abstract:** The development of implantable medical devices is challenging as must be guaranteed their safety, security and functional correctness. Current certification process is based on an open-loop approach, thus not considering the interaction between the pacemaker and the cardiac conduction system. Recently, an automata-based model has been proposed in order to close the loop and tackle this problem. However, as this model does not consider the electrical characteristics of pacemaker and heart signals, hardware-related problems are still a great concern. In this paper, it is introduced a new electrode-tissue interface to extend the existent automata-based model. By closing the loop using the proposed approach, the system can take into consideration new properties such as the energy provided by the pacemaker to stimulate the heart. Thus, based on the strength-duration curve, one can verify if a depolarization event was carried out. Indeed, depolarization of action potentials triggers an intracardiac electrogram generator that controls a voltage source at the electrode-tissue interface, providing the electrical signal to the pacemaker sensing system. This extension allowed to represent the pacemaker sensing, pacing, and battery circuits, as well as to evaluate the real scenario of stimulation and the effects of cardiac electrical parameters on its efficacy. The proposed model enables to include and test the pacemaker hardware specifications and evaluate more realistic scenarios of oversensing, undersensing, and failure-to-capture with a closed-loop heart.

*Keywords:* Electrode-tissue interface, strength-duration curve, closed-loop validation, model-based design, pacemaker, heart modeling.

---

### 1. INTRODUCTION

A cardiac pacemaker (PM) is an electronic medical device used in the treatment of bradycardia. It can be implanted through a minor surgical procedure, positioning its leads in the atrium (upper chamber), ventricle (lower chamber), or both. Once implanted, it allows it to sense the heart's electrical activity and deliver an electrical pulse when needed to synchronize heart functioning. This pulse causes depolarization in the connected region and aims to correct the rhythmic dysfunction detected in the patient's Cardiac Conduction System (CCS). The failure or malfunction of a PM can lead to health damage or even death. Health regulatory agencies, like the Brazilian National Health Surveillance Agency (ANVISA) and the Food and Drugs Administration (FDA), classify this device as "maximum risk" and establish a series of norms and standards, for example, the ISO 14971 and IEC 60601-1, which manufacturers must use to generate evidence of safety, security, and efficacy (Jiang and Mangharam, 2015).

In recent years, a number of recalls associated with pacemaker failures has raised a concern about the current certi-

fication process. Indeed, current standards recommend to evaluate the behavior of a pacemaker using an open-loop approach. Clinical trials are the only certification phase in which it is possible to observe its behavior interacting with a heart (closed-loop). At this stage, due to the inability to control the patient's condition, some cases may not be correctly evaluated. A possible solution is to use a *Model-Based Design* (MBD) technique during the certification process, allowing the biomedical industry to evaluate the interaction between the pacemaker and the heart still in the development phase. In order to do that, we need to model the pacemaker and the Cardiac Conduction System (Ai et al., 2019).

Current PM and CCS models are based on automata (Yip et al., 2016). Essentially, the PM model represents the behavior of the pacemaker's software (SW), and the CCS model reproduces the cardiac electrical dynamics, modeling the generation and the propagation of cardiac electrical impulses. Thus, closed-loop model is event-based and does not fully represent the electrical interface that connects the PM and the heart. From the PM's point of view, the

heart is seen as an electrical impedance in series with a voltage source (Kay and Shepard, 2017). The electrical signal generated by the heart, the intracardiac electrogram (IEGM), is read by the sensing circuits to detect cardiac depolarization events. On the other hand, when the pacemaker detects the need for therapy, a voltage pulse is provided during a certain amount of time. The current drawn from the circuit depends on the impedance of the cardiac tissue and the effectiveness of the stimulation depends on the amount of energy transferred, according to the amplitude-duration curve. Automaton-based models do not consider these characteristics, limiting the analysis and the validation to the pacemaker's SW point of view. A recent study carried out to identify the causes of PM's recalls pointed out that SW-related problems represent 19% of recalls and problems associated with hardware (HW) 67% (Maisel et al., 2001).

In this work, we propose an extension of the CCS model presented in that considers the electrical interface between the PM and the heart. Further, it emulates the characteristics of the electrical signals by using an IEGM generator and considers the amplitude-duration curve to stimulate the heart. We present how the model behaves in the occurrence of sinoatrial node (SA) dysfunction and we use an ideal battery model to demonstrate how the proposed extension contributes to evaluate hardware-related issues, while keeping the advantages provided by automata-based models. Indeed, this method extends the PM's logical model and enable developers to test and evaluate the PM's HW specifications considering a closed-loop approach.

## 2. THE CARDIAC CONDUCTION SYSTEM

The Cardiac Conduction System comprises structures where Action Potentials (AP) are produced and transmitted allowing the heart to contract. The AP is the tension seen by the intra- and extracellular environment due to the concentration of sodium and potassium ions. An action potential has three well-defined states: Rest Period (Rest), Effective Refractory Period (ERP) and Total Refractory Period (TRP). In the Rest state the cell has approximately -90mV. When depolarizing due to stimuli from neighboring cells or external stimulation, this voltage goes to zero and reaches the ERP state. In this state, new stimuli will not change the cell's state. After a while, it reaches the TRP state. In this phase, new stimuli can cause a new depolarization, returning to the ERP state; otherwise, after a certain time the cell is polarized again, ending the cycle. Under normal conditions, the heart spontaneously generates atrial depolarization in the cells of the sinoatrial node (SA) in a rate between 50 to 100 beats per minute (BPM). After this depolarization, the generated AP stimulates neighboring cells by propagating this electrical impulse through the CCS pathway. This propagation takes place long enough for blood to reach the ventricular chamber and be pumped out of the heart with adequate blood pressure.

Arrhythmias represent a dysfunction in the generation and/or propagation of action potentials in the Cardiac Conduction System. For example, SA node dysfunction can cause the heart's natural rhythm to slow down. In this case, a pacemaker connected to the atrial region is

used. It will detect the slow rhythm and provide a voltage pulse for a certain amount of time to achieve a proper heart rate. Atrioventricular (AV) block is characterized by the non-propagation of the electrical impulse in the ventricle. In this case, the device is connected in both cardiac chambers, atrium and ventricle. Upon detecting that the electrical impulse does not reach the ventricle region after an atrial depolarization has occurred, it will provide an electrical stimulus in the ventricle. The action potentials generation and propagation behavior can be captured using the formalism of timed or hybrid automata.

### 2.1 CCS model

The CCS propagation network can be simplified by defining a set of 33 cells and 34 paths interconnecting these cells, as shown in Fig. 1-(a). The circles represent the cells and the black lines represent the AP propagation paths. There are two models to represent the action potential: a) based on timed automaton (TA); and b) based on hybrid automaton (HA). These tools provide enough syntax and semantics to reproduce the generation and propagation of APs. Abstraction provided by TA does not allow to reproduce the morphology of action potential signals. On the other hand, HA-based models allows it. However, both approaches do not consider the electrical coupling interface between the pacemaker and the cardiac conduction system. In this work, we use a timed based automata for simplicity (Jiang et al., 2010). Nevertheless, our proposed extension can be used in both models. In such context, action potentials area modelled by the node automaton and the electrical propagation by the path automaton. These models are discussed below.

*Node automaton* The node automaton used in this work is shown in Fig. 1-(b). It starts in the Rest state and reaches the ERP state if it receives an event or if the timer reaches the value of the parameter  $T_{rest}$ . In the Figure, [event] represents the events generated by the path automaton connected to it or the external stimulation of the PM. It remains in the ERP state during the time interval  $T_{erp}$ . In this state, external stimuli do not generate transitions in the automaton. In the TRP state, if the cell does not receive a new stimulus, the automaton reaches the Rest state after the time defined by  $T_{trp}$ ; otherwise, the automaton returns to the ERP state and the parameter  $T_{erp}$  receives a value that depends on how long the automaton was in the TRP state. Transition conditions are represented between [ ] and actions performed between { }. The syntax and semantics follow the TA formalism (Alur, 1999).

*Path automaton* The Path Automaton connects one or more cells at two distinct nodes. When an event is received, it is propagated after some time to the other node. The automaton can be seen in Fig. 1-(c). The automaton starts in the Idle state. If an Act1 occurs, which represents the occurrence of a stimulation event at one end, it reaches the Ante state, which models the forward propagation time. If an Act2 event occurs, which represents the stimulation at the other end, it reaches the Retro state, which models the propagation time in the opposite direction. In the Ante state, after the time  $T_{ante}$ , the Conflict state is reached. In Retro state, after time  $T_{retro}$ , the Conflict state is also

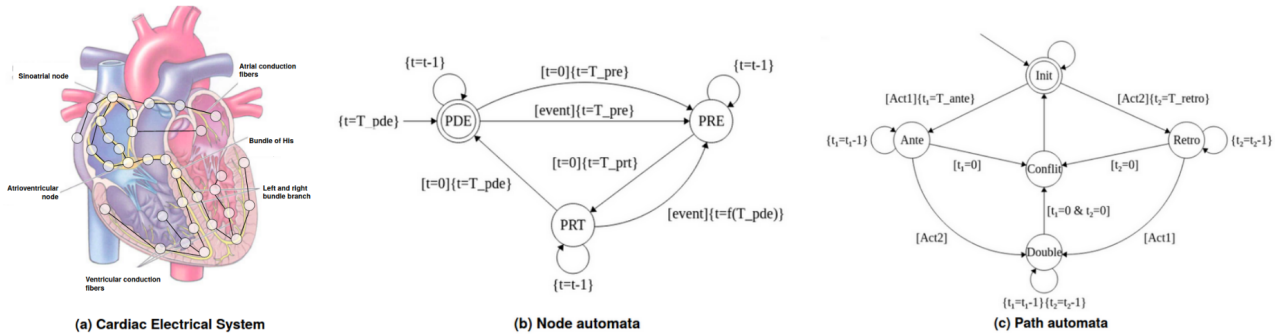


Figure 1. (a) CCS representation. (b) Node automaton. (c) Path automaton.

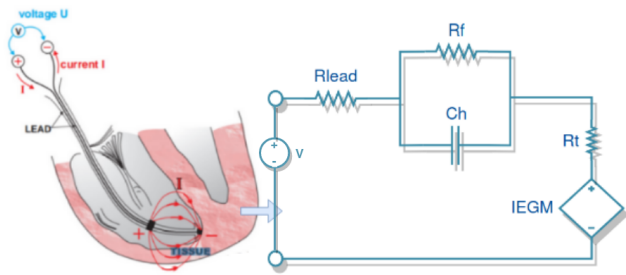


Figure 2. Electrode-tissue interface and model.

reached. In the Ante or Retro state, if Act2 or Act1 occurs, respectively, then the automaton reaches the Double state and remains in it until the timers reach  $T_{ante}$  and  $T_{retro}$ . The Conflict state is made to avoid going back to flow. The feature of propagating in both directions and defining the propagation latency with the parameters  $T_{ante}$  and  $T_{retro}$  makes it possible to create different arrhythmia scenarios.

**Complete CCS model** Arrhythmias are reproduced by configuring the time parameters of these automata. The case of SA node dysfunction, for example, can be represented by adjusting only the SA node parameter. For more complex arrhythmias, we need to adjust parameters of other automata. The interface of this model can be any available cell. In case of bicameral pacemakers, we need to consider both SA and Right Ventricle Apex (RVA) nodes. These cells receive events from the PM logic model and provide the depolarization events. For example, in the case of an AV block, where after a depolarization of the SA node the propagation to the ventricle does not occur, the logical model of the PM receives the event from the SA node but it does not reach the RVA node, even after the expected propagation time. Thus, the PM must provide a pacing event (VP) in the RVA cell, resynchronizing the heart rate. In case of SA node dysfunction, the PM receives the SA node depolarization events. If the next depolarization does not occur in the expected time interval, an atrial pacing (AP) event is performed. This allows evaluating the closed-loop behavior of the pacemaker SW model. However, the sensing signals must be generated by the PM's sensing system from the IEGM signal processing. Further, the pacing events must be generated as a function of the energy level required to perform cardiac stimulation. These mechanisms can be derived with the introduction of the electrode-tissue interface and the amplitude-duration curve.

### 3. ELECTRODE-TISSUE INTERFACE

The connection between the pacemaker and the cardiac tissue is realized by the use of leads, which are insulated cables with electrodes at their ends. From the PM point of view, this connection is seen as a series impedance and a voltage source, as shown in Fig. 2. Typical values are  $R_{lead} = 50\Omega$ ,  $R_f = 80\Omega$  and  $C_h = 3\mu F$ . The  $R_{lead}$  parameter represents the lead wire impedance and ranges from 40 to 80 Ohms. The parameter  $C_h$  is called "Helmholtz-layer" and represents the intrinsic capacitance of the contact between the conductor, with the presence of electrons, and the cardiac tissue, with the presence of  $Na^+$  ions. In parallel to  $C_h$ , there is the resistance  $R_f$ , referred to as "Warburg-resistor", which represents the current flow between the conductor and the myocardium. Finally, the cardiac tissue is represented by pure resistance  $R_t$  (MOND et al., 2014). Values of  $R_t \in [250\Omega, 2500\Omega]$ , values below 250  $\Omega$  indicate isolation break and values above 2500  $\Omega$  indicate lead break. Modern PMs measure this impedance in order to detect such problems (Effert et al., 1975; Wang and Hayes, 2018). The voltage source models the IEGM. The IEGM is characterized by its amplitude, its slew rate and noise due to muscle contractions and external interference. The typical amplitude value is 10 mV. This signal is processed by the sensing circuits to capture depolarization events. A very noisy IEGM can cause oversensing cases, where the pacemaker detects false depolarization events. A low amplitude IEGM can generate undersensing, where the PM does not detect depolarization events. To solve these problems, a pacemaker has a sensitivity parameter that defines the detection threshold. In addition, the sensing system has amplifier circuits, filters and voltage threshold detectors to condition and detect the depolarization events (Silveira and Flandre, 2004).

#### 3.1 Strength-duration curve

The stimulus delivered by a pacemaker is configured in terms of voltage (or current) amplitude and pulse duration. Amplitude can typically range from 0.8-5 V, and pulse duration from 0.05 to 2.0 ms. The amplitude-duration curve relates the pacing threshold and pulse duration in order to stimulate a heart. An example of this curve is shown in Fig. 3. The region over or above the voltage curve provides the values for amplitude and duration of the stimulus at which cardiac tissue is depolarized. The rheobase value represents the lowest voltage that stimulates the myocardium if the pulse duration is infinite. In

other words, voltage values below rheobase will generate failure-to-capture events, in which the pacemaker provides the stimulus, but there is no cardiac depolarization. For practical purposes, the rheobase voltage is typically determined with a pulse duration of 2 ms. Chronaxie is the pulse width twice the rheobase. The most energy-efficient stimulation takes place in the chronaxie.

The strength-duration curve can be constructed using (1), the so called Lapique equation, where  $V_r$  is the rheobase voltage,  $t_c$  the chronaxie width and  $d$  the pulse duration. The stimulation threshold can also be specified in terms of energy. The stimulation energy is given by Eq. 2, where  $V$  is the pulse amplitude,  $d$  the pulse duration and  $R_t$  is the tissue impedance (Kay and Shepard, 2007). Substituting (1) in (2), we obtain Eq. (3) that represents the threshold energy as a function of the rheobase, chronaxie and tissue impedance voltage, which are parameters of the heart. Note that this equation represents the theoretical energy threshold to cause depolarization. However, the actual energy applied by the device depends on the battery conditions, the current drawn by the pacemaker operation and the pacing circuit design. Adding this feature in the automaton-based model allows us to assess the effectiveness of stimulation considering such scenarios.

$$V = V_r \left( 1 + \frac{t_c}{d} \right) \quad (1)$$

$$E = \frac{V^2}{R_t} d \quad (2)$$

$$E_{th} = \frac{[V_r(1 + \frac{t_c}{d})]^2}{R_t} d \quad (3)$$

#### 4. EXTENDED CCS MODEL

The electrode-tissue interface can be inserted as shown in Fig. 4, where  $Z_{lead}$  and  $Z_t$  represent the impedance seen by the pacemaker (see Subsection 3). Coupling this interface with the automaton-based model can be done using the IEGM Generator and Energy Monitor modules. The IEGM Generator receives the depolarization events from the SA node to the atrial region and from the RVA to the ventricle region. From this, you can build an HA that will create an IEGM signal for the controlled voltage

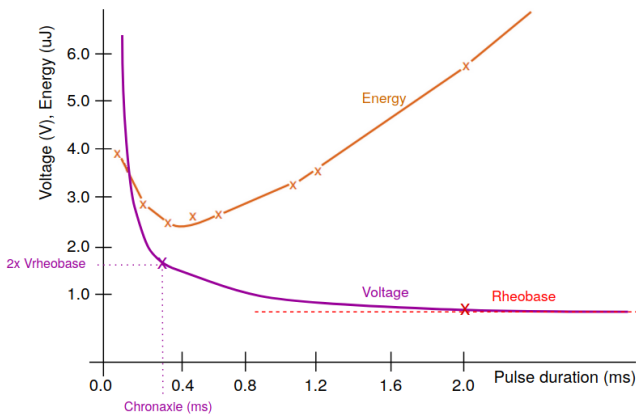


Figure 3. Strength-duration curve example.

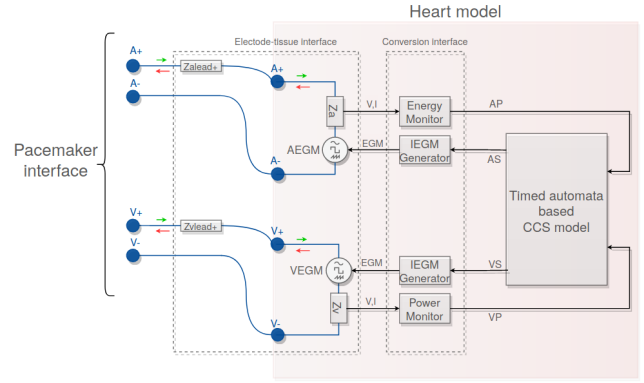


Figure 4. Extended heart model.

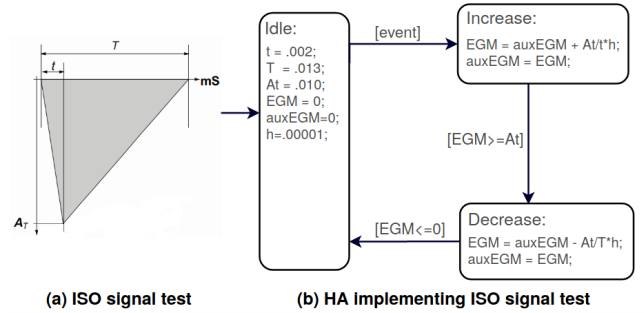


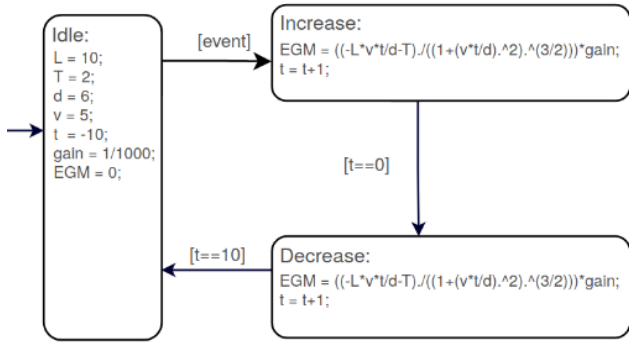
Figure 5. (a) ISO signal test for sensing system. (b) HA implementing standard input test signal.

source. When the pacemaker acts on the heart, the Energy Monitor calculates the transmitted energy and checks whether the stimulus energy is greater than or equal to the energy threshold that causes depolarization, according to Eq. 3. If the stimulus respect such conditions, then a pacing event is generated; otherwise, there is a failure-to-capture event.

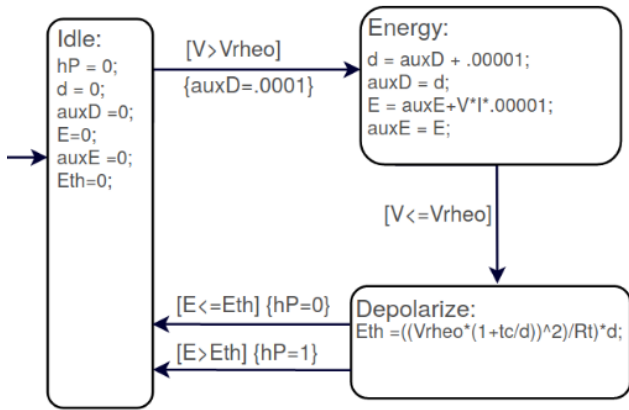
#### 4.1 IEGM generator

The test signal used for the sensing system, as defined by the standard (ISO 14708-2:2016), is shown in Fig. 5-(a). The amplitude  $A_T$  takes values that the device supports and can be negative. The PM parameter that defines the detection threshold is sensitivity. For example, the detection thresholds for the atrium are in the range of 0.2mV to 3.2mV. On the other hand, they are in the range of 0.4mV to 6.4mV for the ventricle. Assuming that the atrial and ventricular sensitivity of a pacemaker is 2 mV and 5 mv, respectively, then every voltage value above that in absolute values must be detected by the PM. The interval  $t$  is 2 ms  $\pm$  0.2 ms and the  $T$  is 15 ms  $\pm$  0.2 ms, which allows to model different slew rates. These allows to better represent an IEGM signal. In this case, we do not consider the noise presented in the signal.

The automaton shown in Fig. 5-(b) represents this curve and is started in the Idle state, where the curve parameters are defined. If an event occurs, then the next state will be Increase, which starts the calculation of the first straight of the test curve. If an event that represents the depolarization of a cell occurs, the next state will be Decrease, which starts the calculation of the first straight of the test curve. The Decrease state is reached when the EGM is equal to



(a) HA implementing IEGM by dipole theory.



(b) HA energy monitor

Figure 6. (a) HA implementing IEGM by dipole theory.  
 (b) HA energy monitor.

or greater than  $A_t$ , then the second part of the line is constructed. The output signal generated is connected to a controlled voltage source that will supply the signal at the electrical interface, as shown in Fig. 4.

The IEGM signal can also be generated by using Eq. 4, proposed by IRNICH (1985). This equation is based on the movement of the dipoles during the propagation of APs due to ions in cardiac tissue.  $L$  is the longitudinal weighting factor of the dipole,  $T$  represents the transverse dipole weighting factor,  $d$  is the distance from the electrode to the myocardium,  $v$  is the propagation velocity and  $t$  is the time. The automaton that implements this function is shown in Fig. 6-(b). In Idle state, the IEGM parameters are set. In the occurrence of an event, the state Increase is reached, where the first part of the curve is computed. Note that the time  $t$  starts with a negative value to generate the initial propagation effect, in this example  $t = [-10 \ 10]$  step-seconds. Still in this state, every instant that the automaton is evaluated, the time is increased until it is reset. In this case, the Decrease state creates the final potential difference of the curve, which is negative until the entire time interval is covered. The results of these signals are presented in Section 5.

$$V(t) = \frac{-Lv\frac{t}{d} - T}{[1 + (v\frac{t}{d})^2]^{\frac{3}{2}}} \quad (4)$$

#### 4.2 Energy Monitor

The depolarization employs the energy transmitted by the pacemaker, and it is implemented by the automaton illustrated in Fig. 6-(b). This automaton receives voltage and current values as input. If the voltage exceeds the rheobase voltage, the automaton reaches the Energy state. Then, the energy of the transmitted pulse is calculated as well as the applied pulse width. Notice that it then remains in this state as long as the stimulus voltage is less than or equal to rheobase. Otherwise, the Depolarize state is reached. In this state the stimulation energy is calculated based on Eq. 3.  $V_{rheo}$ ,  $R_t$  and  $t_C$  are new model parameters and  $d$  is the transmitted pulse width. If the stimulus energy exceeds the  $E_{th}$  threshold, then an hP event is generated, otherwise not. This event is linked back to the automaton-based model, as shown in Fig. 4.

### 5. TEST RESULTS

The extension presented in the previous section was implemented using Simulink software with Simscape and Stateflow packages. To model the electrode-tissue interface, ideal circuit elements were used. The values of  $Z_{lead}$  are presented in Section 3. The  $R_t$  tissue impedance was chosen to be  $500 \ \Omega$ . Automata were implemented with Stateflow. The tests were performed with the IEGM generation and an open-loop cardiac control using an ideal voltage source to validate the cardiac depolarization system as a function of energy. Different voltage and duration values for arrhythmia representations were consistent with theoretical data. In addition, sensing, pacing and battery circuits were placed with an interface that must be connected to the logic model. Our proposed system is shown in Fig. 7.

#### 5.1 IEGM signals and the sensing circuits

Firstly, the generation of IEGM signals was tested and validated. The Cardiac Conduction System model was parameterized for the normal beat. The signals generated by the IEGM Generator automata are presented in Fig. 8: in (a) the IEGM was generated according to ISO 14708-2:2016 and with white noise influence; in (b) the IEGM was generated by the dipole theory as defined in Eq. 4. In the Atrial and Ventricle System block, this signal is connected to an ideal switch and is acquired by a voltmeter as a mean to represent the signal that the sensing system must detect in order to generate the sensing events for the logic unit. Previous works use IEGM morphology generation techniques without considering the system's electrical scenario. The IEGM generator of this model is connected to a controlled voltage source. This allows to observe the current drained from the heart to the MP, which depends on the voltage value of the IEGM and the existent coupling circuits.

#### 5.2 SA node dysfunction

To test the Energy Monitor block, the CCS model was configured to represent SA node dysfunction. The first part of Fig. 9 represents the voltage and current at the system interface indicating a heartbeat at the SA node of 40 BPM.



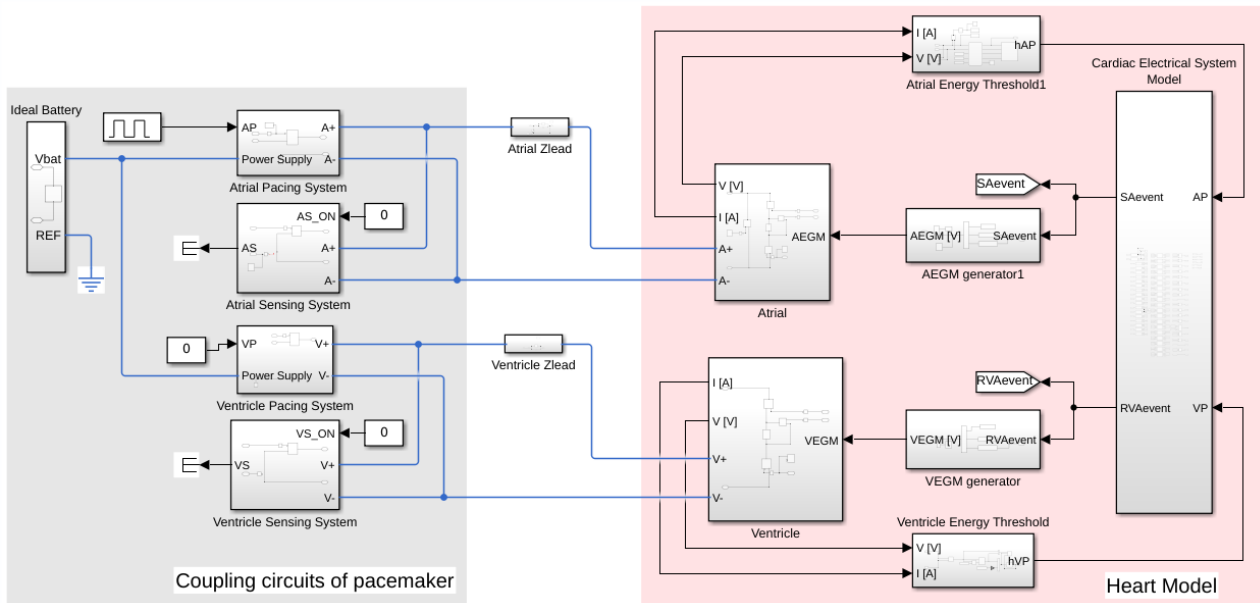


Figure 7. Extension implemented on Simulink.

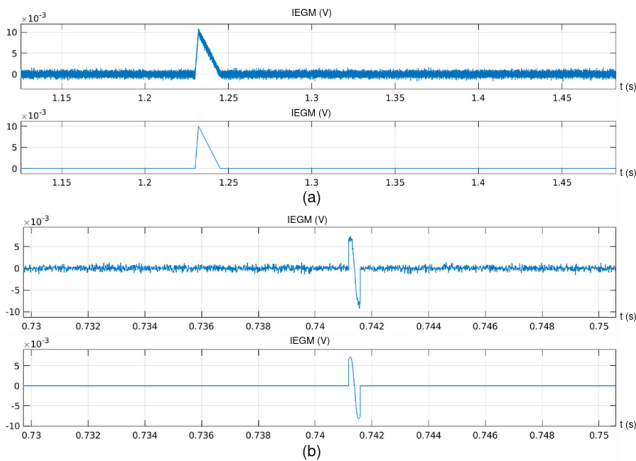


Figure 8. (a) IEGM standard (ISO 14708-2:2016). (b) IEGM dipole theory (Eq. 4).

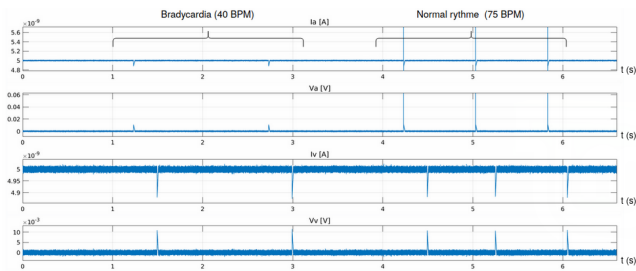


Figure 9. Voltage and current in atrium and ventricle interface.

$I_a$  and  $V_a$  represent the voltage and current read at the interface due to atrial activity. The same is done in the RVA node, to represent the ventricular activity. The time of onset of ventricular activity after atrial depolarization is 0.25 ms, correctly reproducing the case of bradycardia. To correct the heart rhythm, a signal generator was placed to turn an ideal switch on and off in the Atrial Pacing System module. This system is connected to the ideal

voltage source. When the switch is closed, then a voltage pulse with a specific duration is transmitted to the cardiac tissue which is read by the Energy Monitor to verify if this stimulus will generate pacing for the CCS model. The second part of Fig. 9 presents a pacing scenario where the pacemaker activity corrects the heart rate to 75 BPM. The different voltage and duration values that generate failure-to-capture and capture cases are presented below. This model allows to test the stimulation efficacy for different values of the electrical parameters of the electrode-tissue interface. Further, it allows to evaluate the battery models and their discharge behavior.

### 5.3 Depolarization based on energy

The selected parameters to configure the Energy Monitor of the atrial region are:  $R_t = 500 \Omega$ ,  $V_{rheo} = 1.4 \text{ V}$  and  $t_c = 0.3 \text{ ms}$ . Then, one can calculate the depolarization energy curve by (Eq. 3) and the amplitude-duration curve by (Eq. 1) for different pulse duration values. The switches on the sensing systems were opened to turn this system off, as the electrical interface with the heart is shared. Therefore, to apply the pulse, the interface must be available to the pacing system. Points below and above the threshold were chosen, as shown in Fig. 10. It can be seen that for values of amplitude and duration that resulted in energy above or over the curve, the stimulation was achieved. The amplitude-duration curve was also plotted considering the voltage of the stimulation source and the voltage in  $R_t$ . Notice that, due to the lead impedance, there is a drop in the source voltage. Thus, voltage values provided by Eq. 1 must be adjusted considering this drop in order to avoid failure-to-capture. A pulse sample considering 5 V source voltage and 1 ms duration is shown in Fig. 11. It can be seen that there is a drop in the generated voltage in this case. In contrast to previous works, this model allows to observe the behavior of the voltage and current in the coupling interface between MP and the heart. Further, it allows to evaluate the coupling circuits of the device as well as its logical unit represented by a timed automata.

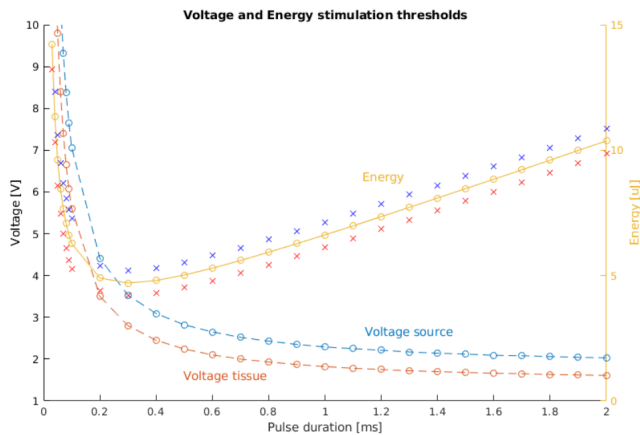


Figure 10. Simulated strength-duration curve. The points in blue indicate values above the stimulation threshold, where there will be cardiac depolarization. On the other hand, the points in red indicate values below the pacing threshold, where there will be no cardiac depolarization or failure-to-capture.

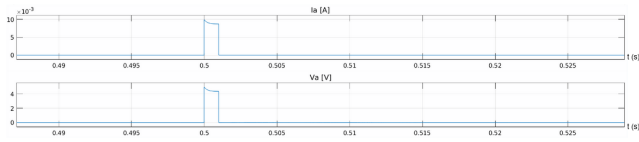


Figure 11. Example of electrical pulse on the interface.

## 6. CONCLUSIONS

In this paper, a new method based on an electrode-tissue interface was proposed in order to model the electrical characteristics of heart and pacemaker signals. The generation of sensing events and pacing effectiveness depends on the pacemaker battery and coupling circuitry, as well as the impedance and pacing characteristics of the cardiac tissue. The proposed method allows to evaluate the pacemaker model considering the hardware and software specifications. Therefore, the device can be submitted to more realistic cardiac conditions and scenarios, reaching the needs of the model-based design. In the most recent researches, CCS models do not represent the electrical coupling interface with pacemakers and do not consider the energy levels provided in cardiac stimulation.

## ACKNOWLEDGMENTS

The authors thank to PPgEE-UFCG, DEE-UFCG, CAPES and CNPq for the award of research grants and study fellowship during the course of these investigations.

## REFERENCES

Ai, W., Patel, N., Roop, P., Malik, A., and Trew, M. (2019). Closing the loop: Validation of implantable cardiac devices with computational heart models. *IEEE Journal of Biomedical and Health Informatics*, 24, 1–1. doi:10.1109/JBHI.2019.2947007.

Alur, R. (1999). Timed automata. In *International Conference on Computer Aided Verification*, 8–22. Springer.

Effert, S., Bisping, H., and Irnich, W. (1975). Clinical requirements for pacemaker therapy. In *Engineering in Medicine*, 3–10. Springer.

IRNICH, W. (1985). Intracardiac electrograms and sensing test signals: Electrophysiological, physical, and technical considerations. *Pacing and Clinical Electrophysiology*, 8(6), 870–888. doi:10.1111/j.1540-8159.1985.tb05907.x. URL <https://doi.org/10.1111/j.1540-8159.1985.tb05907.x>.

ISO 14708-2:2016 (2016). Implants for surgery — active implantable medical devices part 2: Cardiac pacemakers. Standard, International Organization for Standardization, Geneva, CH.

Jiang, Z. and Mangharam, R. (2015). High-confidence medical device software development. *Foundations and Trends in Electronic Design Automation*, 9.

Jiang, Z., Pajic, M., Connolly, A., Dixit, S., and Mangharam, R. (2010). Real-time heart model for implantable cardiac device validation and verification. *2010 22nd Euromicro Conference on Real-Time Systems*, 239–248.

Kay, G. and Shepard, R. (2007). Chapter 1 – cardiac electrical stimulation.

Kay, G.N. and Shepard, R.B. (2017). 3 – stimulation and excitation of cardiac tissues.

Maisel, W., Sweeney, M., Stevenson, W., Ellison, K., and Epstein, L. (2001). Recalls and safety alerts involving pacemakers and implantable cardioverter-defibrillators. *JAMA : the journal of the American Medical Association*, 286, 793–9. doi:10.1001/jama.286.7.793.

MOND, H.G., HELLAND, J.R., STOKES, K., BORNZIN, G.A., and McVENES, R. (2014). The electrode-tissue interface: The revolutionary role of steroid-elution. *Pacing and Clinical Electrophysiology*, 37(9), 1232–1249. doi:https://doi.org/10.1111/pace.12461. URL <https://onlinelibrary.wiley.com/doi/abs/10.1111/pace.12461>.

Silveira, F. and Flandre, D. (2004). *Industrial Implementation of Pacemaker Integrated Circuit in Bulk CMOS Technology*, 25–50. Springer US, Boston, MA. doi:10.1007/978-1-4757-5683-8\_2. URL [https://doi.org/10.1007/978-1-4757-5683-8\\_2](https://doi.org/10.1007/978-1-4757-5683-8_2).

Wang, P.J. and Hayes, D.L. (2018). 119 - implantable pacemakers. In D.P. Zipes, J. Jalife, and W.G. Stevenson (eds.), *Cardiac Electrophysiology: From Cell to Bedside (Seventh Edition)*, 1139 – 1149. Elsevier, seventh edition edition. doi:https://doi.org/10.1016/B978-0-323-44733-1.00119-X. URL <http://www.sciencedirect.com/science/article/pii/B978032344733100119X>.

Yip, E., Andalám, S., Roop, P., Malik, A., Trew, M., Ai, W., and Patel, N. (2016). Towards the emulation of the cardiac conduction system for pacemaker testing. *ACM Transactions on Cyber-Physical Systems*, 2. doi:10.1145/3134845.